

Pertechnetate/Perrhenate-Linked Frameworks of U^{IV}, U^{IV}₆-Hexamer and Uranyl (VI) Building Units

Mohammad Shohel,* Ian Colliard, and May Nyman*



Cite This: *Inorg. Chem.* 2025, 64, 15039–15049



Read Online

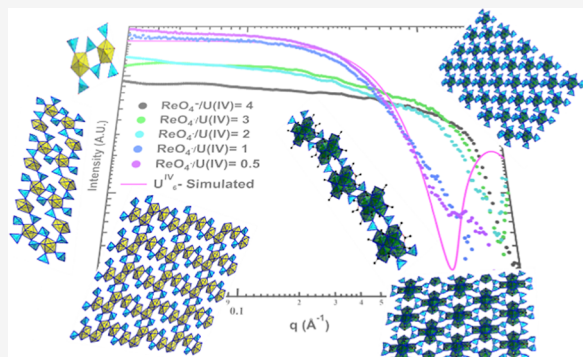
ACCESS |

Metrics & More

Article Recommendations

Supporting Information

ABSTRACT: Uranium-TcO₄⁻ structures enhance understanding of comobility, solid-phase formation, and solution speciation in nuclear materials including spent fuel and wastes. Different solubility and coordination of U(IV) and U(VI) drive their behavior in these complex matrices and in the environment. The present study provides bonding information from 11 U(VI) and U(IV) pertechnetate/perrhenate compounds (ReO₄⁻, nonradioactive surrogate). Reported phases are synthesized from U^{IV}/U^{VI}O₂²⁺ acetate salts and perrhenic/pertechnic acid at room temperature. Single-crystal X-ray diffraction reveals the assembly of U^{IV} and U^{VI}O₂²⁺ into low-dimensional frameworks, linked by pertechnetate/perrhenate. In the series of compounds, nuclearity is dictated by oxoanion to uranium ratio in the reaction solution, as well as corresponding acidity introduced by the pertechnic/perrhenic acid. Higher MO₄⁻:U^{VI}O₂²⁺ (M = Tc, Re) ratios (4:1, 3:1, 2:1) yielded predominantly 1D and 2D networks with no connectivity between uranium polyhedra. Lower ratios (i.e., 1:1) crystallized compounds featuring uranium clusters linked into frameworks by pertechnetate/perrhenate including a tetrameric uranyl clusters for both ReO₄⁻ and TcO₄⁻, and the well-known U^{IV}₆O₄(OH)₄¹²⁺-hexamer (U^{IV}₆) linked by ReO₄⁻. Small-angle X-ray scattering identified assembly of U^{IV}₆ in reaction solutions prior to crystallization. Because U^{IV}₆ is a molecular analogue of UO₂, these structures provide insight into pertechnetate-uranium oxide interactions in nuclear materials.



1. INTRODUCTION

The uranium-235 fission reaction is the most widely exploited for nuclear power plants and is an important component for a sustainable energy future. Technetium-99 is one of the high yield and long-lived decay products from the uranium-235 fission reaction. The dissolution of spent fuel for reprocessing or disposal yields complex mixtures containing uranium, technetium, and other decay products and process chemicals. The speciation and coordination chemistry of both uranium and technetium have evoked interest from researchers due to their relevance in different conditions and environments. For example, the reprocessing of spent nuclear fuel (SNF) depends on speciation of the fission products and how they interact with each other. During reprocessing, the oxoanion of technetium in its most common 7+ oxidation state known as pertechnetate (TcO₄⁻) can pose a major challenge in efficient separation of fission products. The plutonium uranium reduction extraction (PUREX) process has historically been the primary process utilized widely for the reprocessing of SNF. In the PUREX process, the used fuel is first dissolved in nitric acid, followed by extracting actinide cations into a hydrocarbon phase (typically kerosene or n-dodecane) by complexing with TBP.¹ The PUREX process is effective for extracting actinides such as uranium in both +4 and +6 states.² However, it has been noted that TcO₄⁻ coextracts with

actinides and other large cations including zirconium and lanthanides, either as counteranions or by direct bonding between the metal and oxoanion. The bonding between TcO₄⁻ and actinides has also been observed for other extractant media such as monoamide where the pertechnetate coordinates the uranyl cation in a monodentate fashion in the inner coordination sphere.³ To delineate the coextraction mechanism of actinides and pertechnetate, Sarsfield and co-workers have isolated TcO₄⁻/ReO₄⁻ (perrhenate, a nonradioactive surrogate for pertechnetate)-ligated Th(IV), U(IV), and U(VI) complexes which include organophosphorus ligands that are representative of the extractants used in the PUREX process.^{4–6} Their reported structures suggest that the comobility of technetium and actinides is due to the direct coordination of TcO₄⁻ with actinide cations.

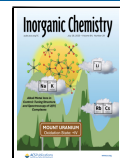
The chemical interplay between technetium and uranium, both with facile redox chemistry, is also relevant for the

Received: April 30, 2025

Revised: June 30, 2025

Accepted: July 8, 2025

Published: July 15, 2025



ACS Publications

© 2025 American Chemical Society

15039

<https://doi.org/10.1021/acs.inorgchem.5c01958>
Inorg. Chem. 2025, 64, 15039–15049

management of legacy waste such as those stored in the Hanford tanks. The redox environments in heterogeneous (containing solids and liquids) legacy wastes vary spatially and temporally, making speciation more diverse and complex. Therefore, the aqueous phase coordination chemistry of technetium species with uranium (and other cations present in aqueous wastes) also warrants study. Fedossev and colleagues studied aqueous phase interactions between Np(V/VI) and Pu(V) with TcO_4^- by vibrational spectroscopy. They isolated only one structure featuring NpO_2^{2+} cations in pentagonal bipyramidal coordination, linked into layers via bridging TcO_4^- .⁷ In 2007, Karimova and Burns crystallized several complexes containing uranyl monomers, dimers, and trimers directly coordinated to ReO_4^- .⁸ In 2022, Decoteau and Polinsky reported two new families of trivalent lanthanide-perrhenate extended structures with varying dimensionality.⁹ In 2024, Strub et al. reported more than 20 structures featuring pertechnetate salts of alkaline earths, transition metals, and lanthanides.¹⁰ Our recent contributions have also expanded the library of metal- $\text{TcO}_4^-/\text{ReO}_4^-$ coordination compounds of both lighter and heavier actinides (Th, U, and Pu)^{11–13} as well as other elements relevant to SNF (Zr, Hf, and Ce).^{12,14} Other than comprehensive bonding information gleaned from isolated structures, we have also performed related solution characterization to deepen our fundamental knowledge of Tc chemistry in the range of relevant complex matrices.^{11,13–15}

Coordination between uranium and pertechnetate/perrhenate is of special interest since uranium is by far the most abundant actinide in nuclear wastes and in SNF. Most prior studies have focused on $\text{UO}_2^{2+}\text{-ReO}_4^-/\text{TcO}_4^-$ compounds, which are less challenging to synthesize than tetravalent uranium compounds since U(IV) is both less stable under ambient conditions and less soluble under aqueous conditions. In Strub's recent periodic table survey, they stated challenges of isolating $\text{U(IV)}\text{-ReO}_4^-/\text{TcO}_4^-$ compounds due to the inability to control redox chemistry.¹⁰ The U(IV) system is of particular interest to actinide chemists due to its propensity to form molecular oxoclusters, perhaps related to the poor solubility, with nuclearity ranging from 6 to as 84 metal centers.^{16–21} Hexanuclear $\text{U}^{\text{IV}}_6\text{O}_4(\text{OH})_4$ (U^{IV}_6) is always the core building unit, also the building block of $\text{U}^{\text{IV}}\text{O}_2$, and readily converts to nanocrystalline- UO_2 in solution.²²

In our present work, we describe the coordination of perrhenate and pertechnetate with both U(VI) and U(IV) via eight $\text{U(VI)}\text{-TcO}_4/\text{ReO}_4$ and three $\text{U(IV)}\text{-ReO}_4$ crystal structures, where structural diversity is accessed by varying the $\text{TcO}_4/\text{ReO}_4\text{:U}$ ratio of the reaction solution. All obtained structures are low-dimensional (1D/2D) frameworks of U^{IV} or $\text{U}^{\text{VI}}\text{O}_2^{2+}$ monomers linked by $\text{TcO}_4/\text{ReO}_4$. Lower ratios of $\text{TcO}_4/\text{ReO}_4\text{:U}$ yielded frameworks of linked oxoclusters for both U^{IV} or $\text{U}^{\text{VI}}\text{O}_2^{2+}$. Most noteworthy is two frameworks featuring ReO_4 -linked U^{IV}_6 oxoclusters, which can enable understanding of UO_2 -pertechnetate association at interfaces, or pertechnetate's role in promoting colloidal UO_2 aggregation. Due to the facile redox behavior of both U^{IV} and Tc, we unfortunately were not able to isolate pristine TcO_4 -linked U^{IV}_6 oxoclusters at this time. Small-angle X-ray scattering (SAXS) studies evidenced the formation of the U^{IV}_6 -hexamers prior to crystallization. Bulk characterization supporting single-crystal X-ray diffraction (SCXRD) for perrhenate analogues included Fourier transform infrared spectroscopy (FTIR), Raman spectroscopy, UV-visible spectroscopy, and powder X-ray diffraction (PXRD). Both pertechnetate and perrhenate

analogues were examined by scanning electron microscopy-energy dispersive spectroscopy (SEM-EDS) for both morphology and composition.

2. EXPERIMENTAL SECTION

2.1. Safety Statement. Caution!! ${}^{99}\text{Tc}$ is a β -emitter and ${}^{238}\text{U}$ is an α -emitter. Experiments were conducted by trained personnel in a licensed research facility designed to perform radiation work. During this work, special precautions were taken toward the handling, monitoring, and disposal of radioactive materials. Tc-containing samples were analyzed only by SCXRD and SEM-EDS to avoid contamination of the shared facilities.

Chemicals in the synthesis, $\text{UO}_2(\text{CH}_3\text{COO})_2\cdot 2\text{H}_2\text{O}$ (SPI), CH_3COOH (Sigma-Aldrich), 30% H_2O_2 (Macron Chemicals), and HReO_4 (Sigma-Aldrich), were used as received. The NH_4TcO_4 was obtained from the Oakridge National Lab. Solutions utilized in this study were prepared by using deionized water (18.2 $\Omega\text{M}\cdot\text{cm}$). $\text{UO}_2(\text{CH}_3\text{COO})_2$ was converted to $\text{U}(\text{CH}_3\text{COO})_4$ by following previously published procedure with slight modification.^{18,23,24} The mechanism was described by Salomone et al. (2014).²⁵

In a typical procedure, 10 g of $\text{UO}_2(\text{CH}_3\text{COO})_2\cdot 2\text{H}_2\text{O}$ was added to a solution that contains 25 mL of glacial acetic acid and 75 mL of ethanol (200 proof). The mixture was then stirred until dissolved followed by filtration. The resulting solution was kept inside an UV chamber for 48 h. The solution turned green and formed green precipitates formulated as $\text{U}(\text{CH}_3\text{COO})_4$. The precipitates were filtered out using the Buchner funnel and washed couple of times with ethanol. The synthesized $\text{U}(\text{CH}_3\text{COO})_4$ was dried and stored promptly in the glovebox.

HTcO_4 was prepared by our previously published method.¹¹ In a typical synthesis, the as-received NH_4TcO_4 was added to water and then refluxed until boiling. Then, 30% H_2O_2 was added dropwise in the boiling mixture to convert TcO_2 impurities into TcO_4^- . The resulting clear 0.5 M NH_4TcO_4 solution was passed through a Dowex 50WX8–100 cation exchange resin. The HTcO_4 eluate was collected and stored inside an airtight scintillation glass vial.

2.2. Synthesis of $[(\text{UO}_2)(\text{ReO}_4)_2(\text{H}_2\text{O})] (\text{U}^{\text{VI}}\text{Re}_2\text{-}2\text{D-1})$ and $[(\text{UO}_2)(\text{TcO}_4)_2(\text{H}_2\text{O})] (\text{U}^{\text{VI}}\text{Tc}_2\text{-}2\text{D-1})$. Uranyl acetate solution (0.12 M, 100 μL , 12 μmol) was combined with a 0.12 M perrhenic acid/pertechnic acid solution (300–400 μL , 36–48 μmol) in a 4 mL glass scintillation vial. Evaporating this solution at room temperature for 14 days yielded yellow-colored blocky crystals of $\text{U}^{\text{VI}}\text{Re}_2\text{-}2\text{D-1}/\text{U}^{\text{VI}}\text{Tc}_2\text{-}2\text{D-1}$. The yield of the $\text{U}^{\text{VI}}\text{Re}_2\text{-}2\text{D-1}$ crystalline materials based on uranium was ~76%. The yield of $\text{U}^{\text{VI}}\text{Tc}_2\text{-}2\text{D-1}$ or other Tc-99 containing crystals later described was not measured to avoid radioactive contamination.

2.3. Synthesis of $[(\text{UO}_2)_2(\text{ReO}_4)_4(\text{H}_2\text{O})_3] (\text{U}^{\text{VI}}\text{Re}_2\text{-Chain})$, $[(\text{UO}_2)_2(\text{ReO}_4)_4(\text{H}_2\text{O})_3] (\text{U}^{\text{VI}}\text{Tc}_2\text{-Chain})$, and $[(\text{UO}_2)_2(\text{ReO}_4)_3(\text{H}_2\text{O})]\cdot 2.5 \text{ H}_2\text{O} (\text{U}^{\text{VI}}\text{Re}_3)$. Uranyl acetate solution (0.12 M, 200 μL , 24 μmol) was combined with 0.12 M perrhenic acid/pertechnic acid solution (400 μL , 48 μmol) in a 4 mL glass scintillation vial. Evaporating this solution at room temperature for 10 days resulted in yellow blocky crystals of $\text{U}^{\text{VI}}\text{Re}_2\text{-chain}/\text{U}^{\text{VI}}\text{Tc}_2\text{-chain}$. In the perrhenic acid solution, the minor phase of $\text{U}^{\text{VI}}\text{Re}_3$ also appeared as rodlike yellowish-orange crystals alongside with $\text{U}^{\text{VI}}\text{Re}_2\text{-chain}$. The yield of bulk crystalline material based on uranium was 80%.

2.4. Synthesis of $[(\text{UO}_2)_4(\text{OH})_4(\text{ReO}_4)_4(\text{H}_2\text{O})_4] [\text{U}^{\text{VI}}\text{Re-2D}]$. Uranyl acetate solution (0.12 M, 200 μL , 24 μmol) was combined with 0.12 M perrhenic acid solution (200 μL , 24 μmol) in a 4 mL glass scintillation vial. Evaporating this solution at room temperature for 7 days resulted in block-like yellow crystals of $\text{U}^{\text{VI}}\text{Re-2D}$. The yield of the crystalline materials based on uranium was 70%.

2.5. Synthesis of $[(\text{UO}_2)_4(\text{TcO}_4)_4(\text{H}_2\text{O})] (\text{U}^{\text{VI}}\text{Tc}_2\text{-2D-2})$ and $[(\text{UO}_2)_4(\text{OH})_4(\text{TcO}_4)_4(\text{H}_2\text{O})] (\text{U}^{\text{VI}}\text{Tc-2D})$. Uranyl acetate solution (0.12 M, 200 μL , 24 μmol) was combined with 0.12 M pertechnic acid solution (200 μL , 24 μmol) in a 4 mL glass scintillation vial. Evaporating this solution at room temperature for 10 days led to the

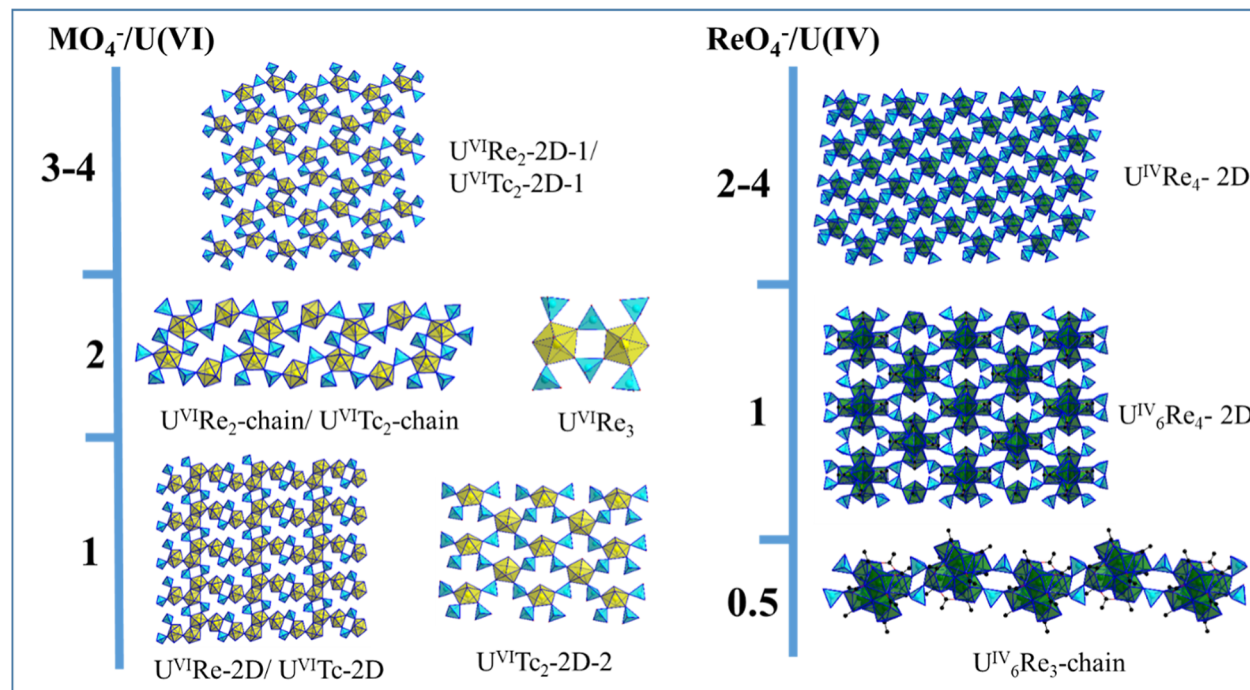


Figure 1. Summary of reaction conditions and topologies obtained from $\text{U}(\text{VI})/\text{U}(\text{IV})$ and $\text{HReO}_4^-/\text{HTcO}_4^-$ reaction solutions. Yellow polyhedra is $\text{U}(\text{VI})$, green polyhedra is $\text{U}(\text{IV})$, and turquoise tetrahedra is ReO_4^- and/or TcO_4^- (as labeled for individual structures). Hydrogen atoms are omitted for clarity.

formation of yellow plate-like crystals of $\text{UVIRe}_{-2\text{D}}$ along with yellowish-orange block-like crystals of $\text{UVTc}_{-2\text{D}}$.

2.6. Synthesis of $[\text{U}(\text{ReO}_4)_4(\text{H}_2\text{O})_3]$ (UIVRe_4-2D). Uranium(IV) acetate (60 mg, 125 μmol) was dissolved with 0.5 M perrhenic acid solution (0.5–1 mL, 500–250 μmol) in a 4 mL glass scintillation vial inside a glovebox under an inert environment. Evaporating this solution at room temperature for 7 days resulted in rod shape green-colored crystals of UIVRe_4-2D . The yield of the crystalline materials based on uranium was 85–90%.

2.7. Synthesis of $[\text{U}_6\text{O}_4(\text{OH})_4(\text{ReO}_4)_4(\text{CH}_3\text{COO})_8(\text{H}_2\text{O})_4]\cdot6\text{H}_2\text{O}$ ($\text{UIV}_6\text{Re}_4-2\text{D}$). Uranium(IV) acetate (120 mg, 250 μmol) was dissolved with 0.5 M perrhenic acid solution (0.5 mL, 250 μmol) in a 4 mL glass scintillation vial inside a glovebox under an inert environment. Evaporating this solution at room temperature inside glovebox for 5 days resulted in rod-shaped dark green crystals of $\text{UIV}_6\text{Re}_4-2\text{D}$. The yield of the crystalline materials based on uranium was 75%.

2.8. Synthesis of $[\text{U}_6\text{O}_4(\text{OH})_4(\text{ReO}_4)_2(\text{CH}_3\text{COO})_9(\text{H}_2\text{O})_4]\cdot(\text{ReO}_4)\cdot5.5\text{H}_2\text{O}$ (UIV_6Re_3- Chain). Uranium(IV) acetate (120 mg, 250 μmol) was dissolved with 0.20 M perrhenic acid solution (0.625 mL, 125 μmol) in a 4 mL glass scintillation vial inside a glovebox under an inert environment. Evaporating this solution at room temperature inside glovebox for 7 days resulted in rod-shaped dark green crystals of UIV_6Re_3- 2D. The yield of the crystalline materials based on uranium was 70%.

2.9. Single-Crystal X-ray Diffraction. SCXRD experiments were performed on a Rigaku Oxford Synergy system equipped with a PhotonJet Cu/Mo source ($\lambda = 1.54178/0.7107 \text{ \AA}$) and hyPix-6000HE photon counting detector. The data were collected at cryogenic temperature (150 K–223 K) and then processed using CrysAlisPro_171.40_64.53 (Rigaku Oxford Diffraction, 2018).²⁶ Analytical absorption and empirical absorption (spherical harmonic, image scaling, detector scaling) corrections were applied after integrating all diffraction frames.²⁷ The structures were solved by the intrinsic phasing method from SHELXT²⁸ program, developed by successive difference Fourier syntheses, and refined by full-matrix least-squares on all F2 data using SHELX²⁹ in the OLEX2 interface.³⁰ The selected crystallographic information for the isolated structures is in Supporting Information (Table S1). The crystallographic

information files of the refined structures can be requested with their deposition number 2445905–2445915 in Cambridge crystallographic data center|Cambridge Crystallographic data centre (CCDC) website.

2.10. Small-Angle X-ray Scattering. SAXS experiments were conducted in an Anton Paar SAXSess instrument using $\text{Cu K}\alpha$ radiation (1.54 \AA) equipped with line collimation. A 2-D image plate was used for data collection in the $q = 0.018\text{--}2.5 \text{ \AA}^{-1}$ range. The lower Q resolution is limited by the beam attenuator. Then SAXS samples were filtered out using a 0.45 μm membrane filter and filled inside 1.5 mm glass capillaries (Hampton Research) to collect SAXS data. Scattering data of neat solvent were also collected for background subtraction. Scattering was measured for 30 min in each experiment. SAXSQUANT software was used for data collection and post processing (normalization, primary beam removal, background subtraction, desmearing, and smoothing to remove the extra noise created by the desmearing routine). IRENA macros with IgorPro 6.3 (WaveMetrics) software was used to analyze the data.³¹ Simulated scattering patterns of the UIV_6 cluster were generated using SolX utilizing structural files (xyz) containing the selected portion of the structure without solvent or coordinated ligands.³²

2.11. Fourier Transform Infrared Spectroscopy. A PerkinElmer Spectrum Two Spectrometer system equipped with a LiTaO_3 MIR detector was used to collect the spectra. The spectra were collected in the scan range from 4000 to 400 cm^{-1} at a resolution of 4 cm^{-1} .

2.12. Powder X-ray Diffraction. The PXRD analysis was carried out by using a Rigaku Miniflex diffractometer with $\text{Cu K}\alpha$ ($\lambda = 1.54056 \text{ \AA}$) from 5° to $50^\circ 2\theta$ at a rate of $2.5^\circ \text{ min}^{-1}$. The air-dried samples were crushed into a powder before analysis. A silicon zero diffraction plate was used as the sample holder when collecting the diffraction data.

2.13. Scanning Electron Microscopy-Energy-Dispersive Spectroscopy. SEM analysis was carried out in a FEI Quanta 600F SEM system which carried out energy-dispersive spectroscopy (EDS) through a $10 \text{ mm}^2 \text{ Si(Li)}$ detector (EDAX inc). The crystalline materials were fixed on a carbon conductive prior to the analysis. The analyses were performed under high vacuum using accelerating voltage 15–30 kV for SEM and 30 kV for EDS analysis.

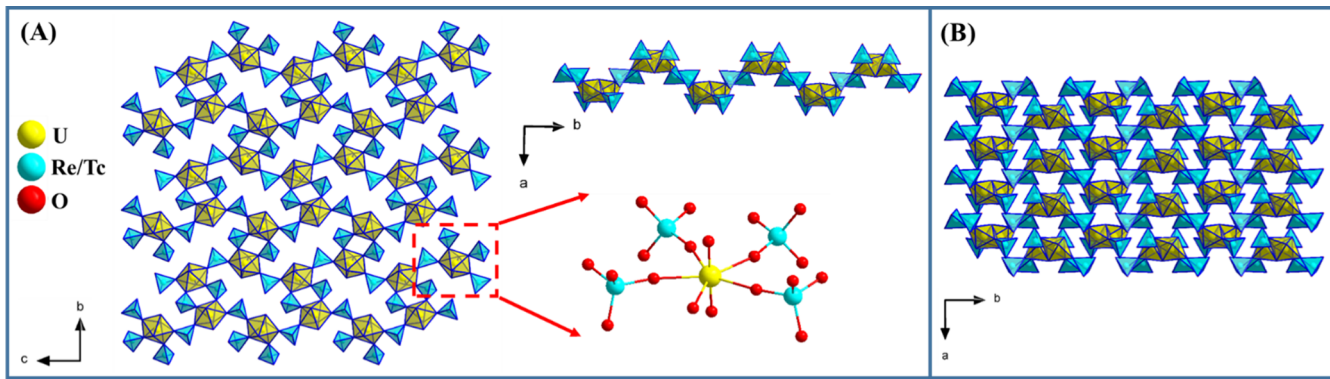


Figure 2. (A) Polyhedral representation of the 2D framework $\text{UVIRe}_2\text{-} 2\text{D-1}$ and $\text{UVITc}_2\text{-} 2\text{D-1}$ viewed along different crystallographic axes. Upper right view down the c -axis shows corrugation of the layers. The ball-and-stick model exhibits the coordination environment of U(VI). (B) View down the c -axis highlighting the stacking of the layers in the a -direction.

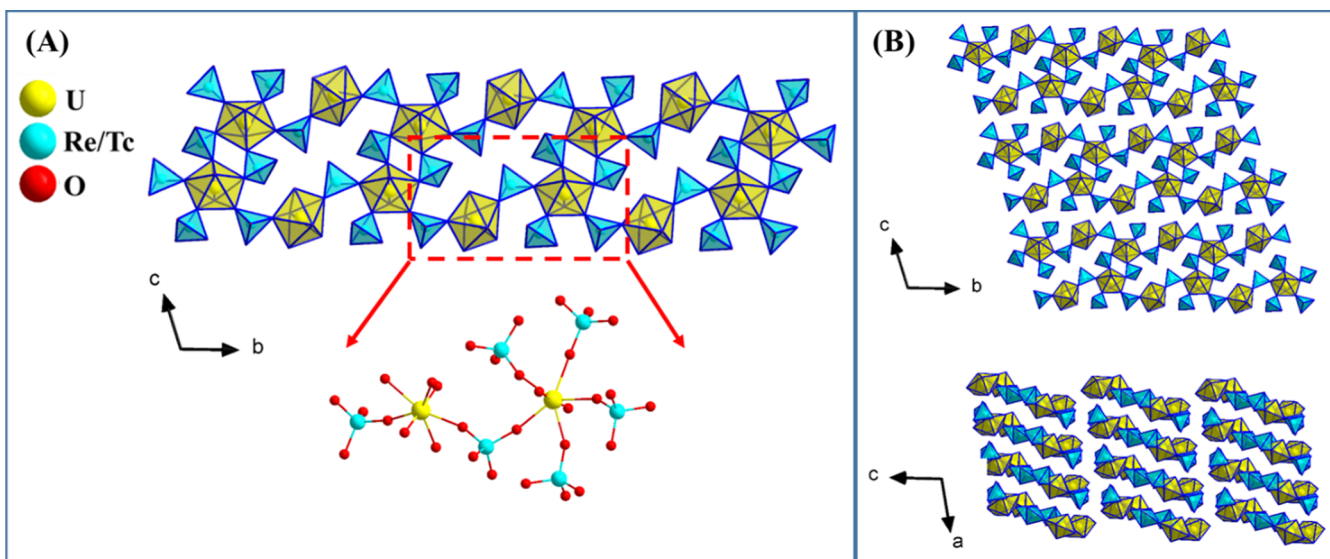


Figure 3. (A) Polyhedral representation of 1D chain $\text{UVIRe}_2\text{- chain}$ and $\text{UVITc}_2\text{- chain}$. The ball-and-stick model exhibits the coordination environment of U(VI). (B) View down the a -axis highlighting the stacking of the layers in the a -direction.

2.14. Raman Spectroscopy. The Raman spectra of air-dried crystalline materials were collected using a Thermo Scientific DXR spectrometer with a 760 nm laser source between wavelengths of 200 and 2000 cm^{-1} .

2.15. UV–Visible Spectroscopy. The UV–visible absorbance of mother liquors inside quartz cuvette was collected using a PerkinElmer UV–visible spectrometer at wavelength 200–800 nm.

3. RESULTS AND DISCUSSION

3.1. Synthesis of Crystalline Material. Our synthetic strategy to probe the coordination of MO_4^- ($\text{M} = \text{Tc}/\text{Re}$) with U(VI)/U(IV) was based on our previous work involving Th(IV) with some modifications.¹¹ In the case of Th(IV), we converted the metal salt solution into hydroxide precipitate by addition of base and then redissolved it with $\text{HTcO}_4/\text{HReO}_4$ at different metal to oxoanion ratios. This strategy was chosen to avoid cations/anions in the reaction mixture that can compete with $\text{ReO}_4^-/\text{TcO}_4^-$ for thorium coordination. However, addition of base in U(IV)/U(VI) salt resulted in a black precipitate of uranium oxide, which was sparingly soluble in $\text{HTcO}_4/\text{HReO}_4$. Evaporation of the supernatant crystallized out a phase that has already been reported.^{7,8} Alternatively, we used the U(IV)/U(VI) acetate salt directly for synthesis

without prior conversion to the hydroxide. The presence of acetate in the reaction mixture did not hinder coordination of $\text{TcO}_4^-/\text{ReO}_4^-$ with U(IV)/U(IV). However, some of the isolated structures contain both acetate and $\text{TcO}_4^-/\text{ReO}_4^-$ coordinated to the metal center.

Figure 1 summarizes the structural topology and phases of isolated structures from syntheses. The overview of the synthesis conditions and topologies obtained is discussed here, while structure details are described below. For U(VI), we carry out synthesis with $\text{MO}_4^-/\text{U(VI)}$ ratio from 4 to 1 in this study and 0.5 in the previously published work.¹³ At ratios higher than charge balance (>2), we synthesized isostructural 2D framework compounds of UO_2^{2+} ($\text{UVIRe}_2\text{-} 2\text{D-1}$ and $\text{UVITc}_2\text{-} 2\text{D-1}$) for $\text{TcO}_4^-/\text{ReO}_4^-$. At a ratio of 2 (equal to charge balance), isostructural 1D chains ($\text{UVIRe}_2\text{- chain}$ and $\text{UVITc}_2\text{- chain}$) were obtained for $\text{TcO}_4^-/\text{ReO}_4^-$, in addition to dimeric molecular cluster (UVIRe_3) of UO_2^{2+} bridged by ReO_4^- . At a ratio of 1, a 2D framework ($\text{UVIRe-} 2\text{D}$ and $\text{UVITc-} 2\text{D}$) containing uranyl tetramer building units was obtained for $\text{TcO}_4^-/\text{ReO}_4^-$. The same ratio also gave a different 2D framework ($\text{UVITc}_2\text{-} 2\text{D-2}$) of UO_2^{2+} monomers for TcO_4^- only. Previously with a 0.5 ratio, we isolated some unique tetrameric/pentameric uranyl molecular clusters that

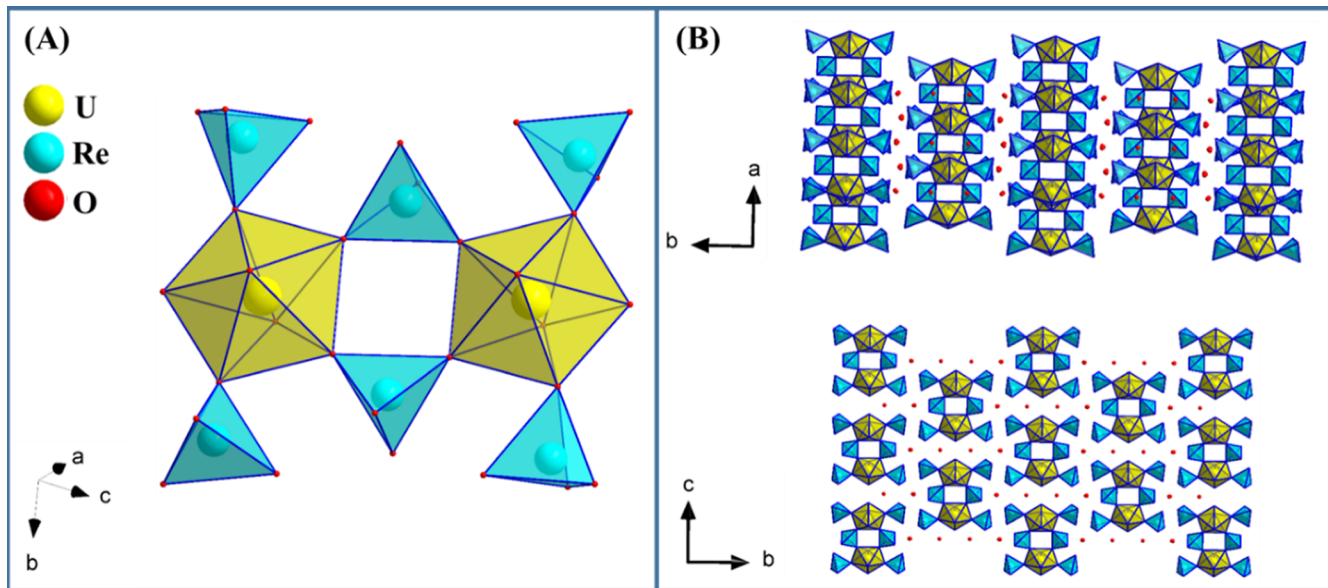


Figure 4. (A) Polyhedral representation of the $\text{U}^{\text{VI}}\text{Re}_3$ molecular cluster. (B) View down the *c*-axis highlighting the stacking of the layers in the *c*-direction.

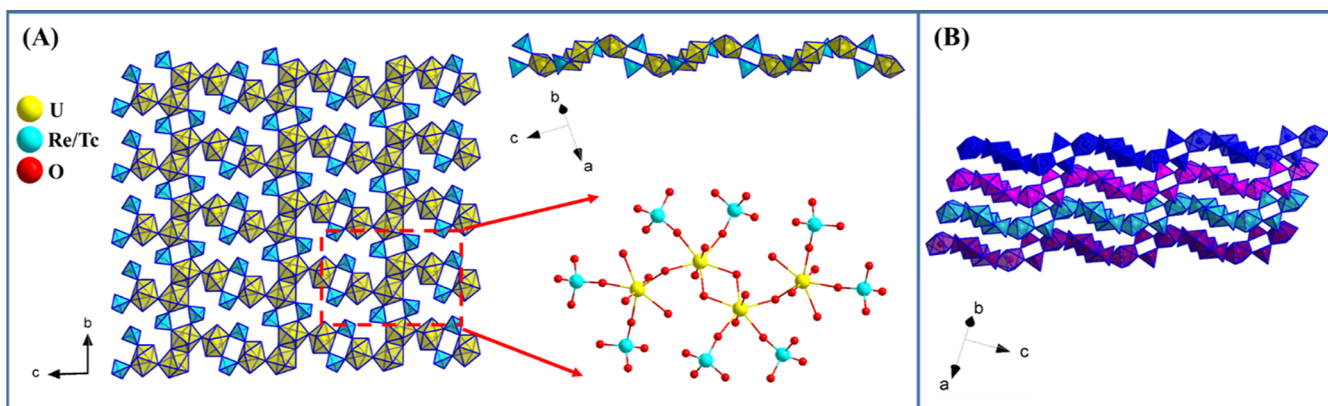


Figure 5. (A) Polyhedral representation of 2D framework $\text{U}^{\text{VI}}\text{Re}_2$ -2D and $\text{U}^{\text{VI}}\text{Tc}_2$ -2D viewed from different crystallographic planes. The ball-and-stick model exhibits the coordination environment of U(VI). (B) Distinguishing the stacked layers by using different colors for adjacent layers.

are coordinated by $\text{TcO}_4^-/\text{ReO}_4^-/\text{Tc(V)}$ and acetate.¹³ For U(IV), we also carried out synthesis with $\text{ReO}_4^-/\text{U(IV)}$ ratios from 4 to 1. At ratios of 2–4, a 2D framework ($\text{U}^{\text{IV}}\text{Re}_4$ -2D) of U(IV) monomers coordinated to ReO_4^- has been isolated. At a ratio of 1, a different 2D framework ($\text{U}^{\text{IV}}_6\text{Re}_4$ -2D) containing ReO_4^- -linked U^{IV}_6 hexamers was crystallized. This same hexamer building block formed a 1D chain ($\text{U}^{\text{IV}}_6\text{Re}_3$ -chain) at a ratio of 0.5. We attempted to synthesize the Tc analogues of these U(IV)- ReO_4^- compounds following the same synthetic procedure. However, addition of pertechnic acid to uranium(IV) acetate yielded an insoluble black precipitate with a light yellow supernatant, suggesting reduction of TcO_4^- to TcO_2 and oxidation of U(IV) to U(VI).

3.2. Structural Description. **3.2.1. $\text{U}(\text{VI})\text{-ReO}_4^-/\text{TcO}_4^-$ Structures.** The isolated U(VI) compounds in this study contain a UO_2^{2+} cation coordinated by five oxygens from oxoanions ($\text{ReO}_4^-/\text{TcO}_4^-$) and/or water molecules in their equatorial plane to form a pentagonal bipyramidal. The average uranium to oxygen distance in the axial direction ($\text{U} = \text{O}_{\text{yl}}$) is $1.7285(11)$ – $1.7731(12)$ Å, and average uranium to oxygen distance in equatorial plane ($\text{U} - \text{O}_{\text{eq}}$) ranges from $2.3335(25)$ – $2.4668(74)$ Å. The $\text{ReO}_4^-/\text{TcO}_4^-$ tetrahedra

have an average M–O distance ranging from $1.6877(10)$ to $1.7497(18)$ Å.

$\text{U}^{\text{VI}}\text{Re}_2$ -2D-1 and $\text{U}^{\text{VI}}\text{Tc}_2$ -2D-1 (Figure 2) are isostructural 2D frameworks with a moiety formula $(\text{UO}_2)(\text{MO}_4)_2(\text{H}_2\text{O})$, where M = Re/Tc. Each UO_2^{2+} unit is coordinated by four $\text{ReO}_4^-/\text{TcO}_4^-$ molecules and a water molecule in the equatorial plane. All of the $\text{ReO}_4^-/\text{TcO}_4^-$ are coordinated to neighboring uranyl ions in the *bc* plane to form the 2D framework. This leads to corrugated layers in the *bc* plane that stack along the *a*-axis.

$\text{U}^{\text{VI}}\text{Re}_2$ -chain and $\text{U}^{\text{VI}}\text{Tc}_2$ -chain are isostructural with a moiety formula of $(\text{UO}_2)_2(\text{MO}_4)_4(\text{H}_2\text{O})_3$, where M = Re/Tc. The chain is composed of two crystallographically distinct UO_2^{2+} sites. The first UO_2^{2+} site is coordinated by five $\text{ReO}_4^-/\text{TcO}_4^-$, among which four are bridging and one is terminal (Figure 3A). On the other hand, second UO_2^{2+} site is coordinated by two bridging $\text{ReO}_4^-/\text{TcO}_4^-$ and three water molecules. The chains extend along the [010] direction and stack on top of each other along the *a* axis. The $\text{U}^{\text{VI}}\text{Re}_2$ -chain has been reported previously by Karimova and Burns.⁸ The Np(VI)-Tc analogue of this chain has also been isolated by Fedosseev et al. (2003).⁷

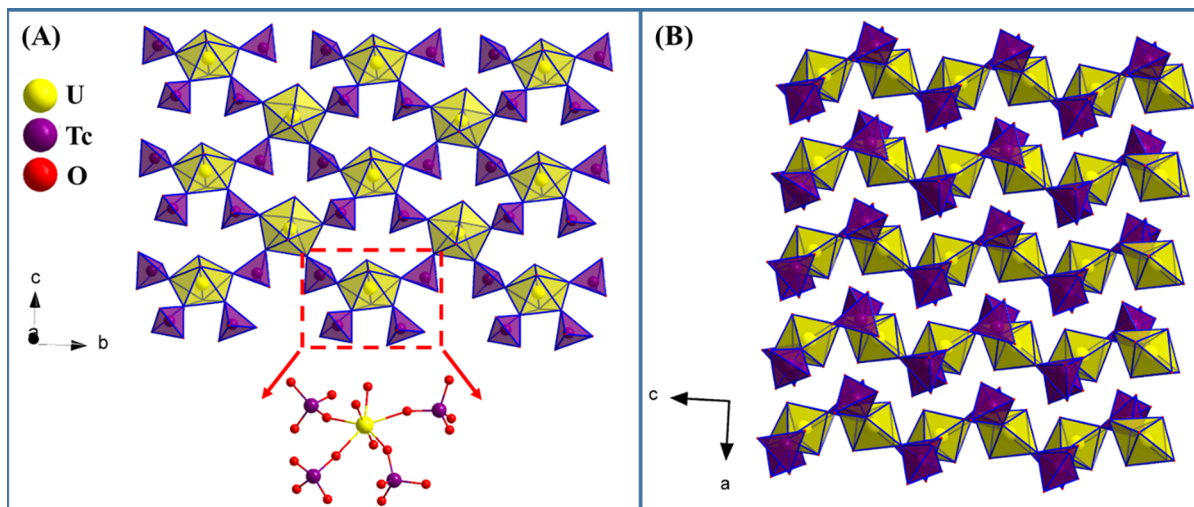


Figure 6. (A) Polyhedral representation of 2D framework $\text{UVI Tc}_2^- \cdot 2\text{D}-2$ viewed from different crystallographic directions. The ball-and-stick model exhibits the coordination environment of U(VI). (B) View down the *a*-axis highlighting the stacking of the layers in the *a*-direction.

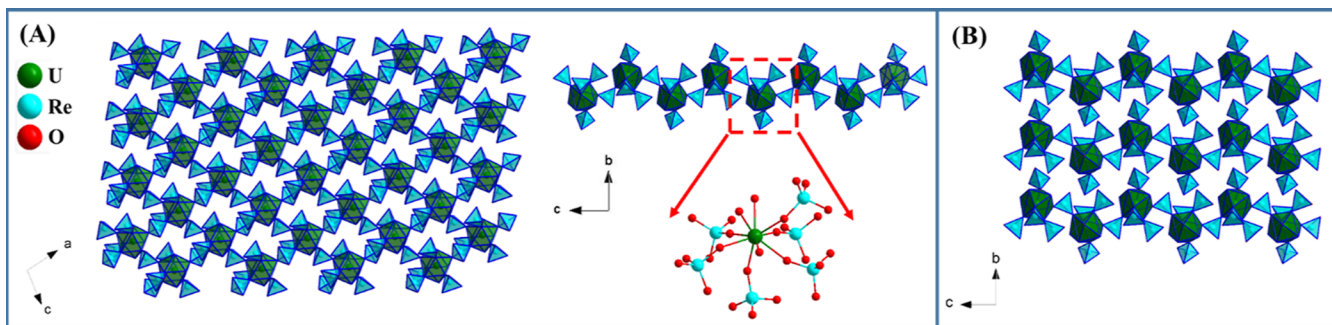


Figure 7. (A) Polyhedral representation of the 2D framework $\text{UVI Re}_4^- \cdot 2\text{D}$ viewed from different crystallographic planes. The ball-and-stick model exhibits the coordination environment of U(IV). (B) View down the *a*-axis highlights the stacking of the layers in the *b*-direction.

UVI Re_3 is a molecular cluster with a moiety formula $(\text{UO}_2)(\text{ReO}_4)_3(\text{H}_3\text{O})$. In this molecular cluster, two UO_2^{2+} units are connected by two bridging ReO_4^- to form a UVI^- dimer (Figure 4A). Each of the UO_2^{2+} units is additionally coordinated by two terminal ReO_4^- and one water molecule in their equatorial plane. Figure 4B shows the arrangement of the molecular clusters in the lattice and their stacking along the *a*-axis. Lattice oxygens, most likely H_3O^+ necessary for charge-balance from the acidic crystallization environment, are present in the lattice. These form a hydrogen-bonded network with nearby oxygens from ReO_4^- or H_2O connected to the UO_2^{2+} unit. The average O–O distance of H-bonded moieties range between 2.6895(11) and 2.8492(23) Å. UVI Re_3 was reported prior as the building unit of an extended 2D framework by Karimova and Burns.⁸ This cluster can also be identified in the UVI Re_2^- chain and UVI Tc_2^- chain structures described earlier. This suggests that UVI Re_3 is an intermediate phase toward assembly of the extended UVI Re_2^- chain. Dimeric uranyl complexes with bridging perrhenate have been isolated earlier by John et al. in 2007 with additional coordination of organophosphate ligands.⁶ It is notable that we have been able to isolate this intermediate phase as a molecular cluster without the presence of any organic ligands in the structure. It is also a testament to the $\text{ReO}_4^-/\text{TcO}_4^-$ oxoanion as a terminal ligand.

UVI Re-2D and UVI Tc-2D are extended 2D framework compounds with a moiety formula of $(\text{UO}_2)_4(\text{OH})_4(\text{MO}_4)_4(\text{H}_2\text{O})_4$, where M = Re/Tc. The

building block of this 2D framework is a tetrameric UVI^- cluster (Figure 5A). The tetramer consists of two UO_2^{2+} units connected to each other by two $\mu_2-\text{OH}$ bonds with U–OH lengths ranging from 2.3423 (12)–2.3728 (11) Å.³³ Each of UO_2^{2+} is connected to an additional UO_2^{2+} by a single $\mu_2-\text{OH}$ bond with U–OH lengths ranging from 2.2925 (13) to 2.3423 (18) Å. The UO_2^{2+} units are additionally connected to bridging $\text{ReO}_4^-/\text{TcO}_4^-$ and H_2O . The $\text{ReO}_4^-/\text{TcO}_4^-$ connects the tetramers along the *bc* plane to form a 2D framework. The layers stack on top of each other along the *a* direction (Figure 5B).

$\text{UVI Tc}_2^- \cdot 2\text{D-2}$ is a 2D framework compound with the moiety formula $(\text{UO}_2)(\text{TcO}_4)_2(\text{H}_2\text{O})$. In the framework, each UO_2^{2+} is coordinated by four bridging TcO_4^- and one H_2O atom (Figure 6A). The bridging TcO_4^- ligands connect the UO_2^{2+} units in the lattice along the *bc* plane. This leads to corrugated layers of frameworks in the *bc* plane, which then stack on top of each other along the *a*-direction.

In case of the U(VI) system and other tri/trivalent cations,^{11,12,14} ReO_4^- appears to be a good surrogate for TcO_4^- since we have been able to synthesize their isostructures. This is not the case for U(IV), which is more redox sensitive. The comparison between Re–O and Tc–O bond lengths in isolated structures has been summarized in Supporting Information (Table S2a,b).

3.2.2. U(IV)-ReO_4^- Structures. $\text{UVI Re}_4^- \cdot 2\text{D}$ is a 2D framework compound with the moiety formula U-

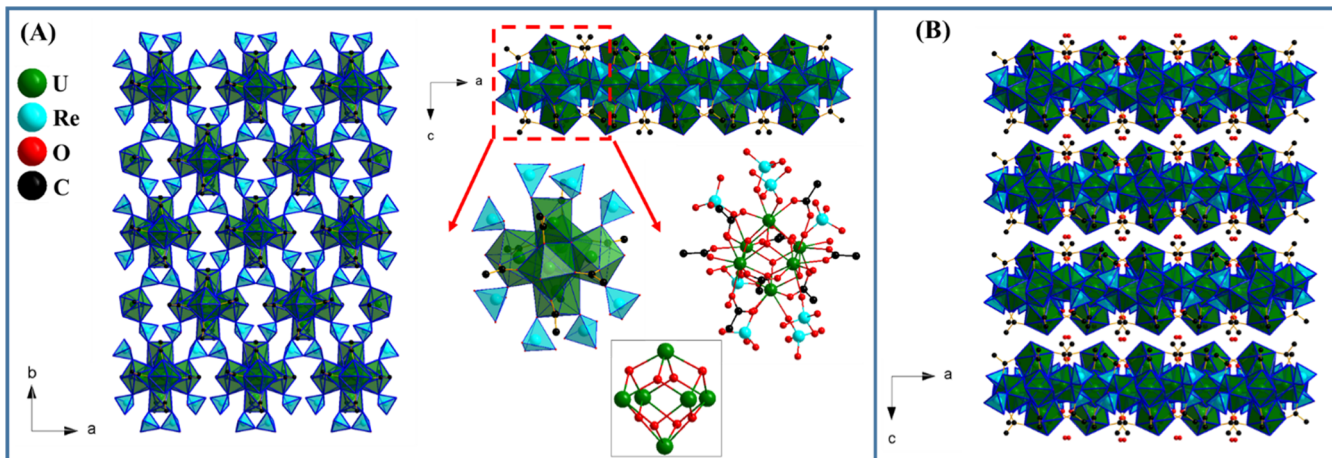


Figure 8. (A) Polyhedral representation of 2D framework $\text{U}^{\text{IV}}_6\text{Re}_4^-$ 2D viewed from different crystallographic planes. The polyhedral and ball-and-stick model exhibit coordination around the U^{IV}_6 unit and its core (inset). Hydrogen atoms are omitted for clarity. (B) View down the b -axis highlighting the stacking of the layers in the c -direction.

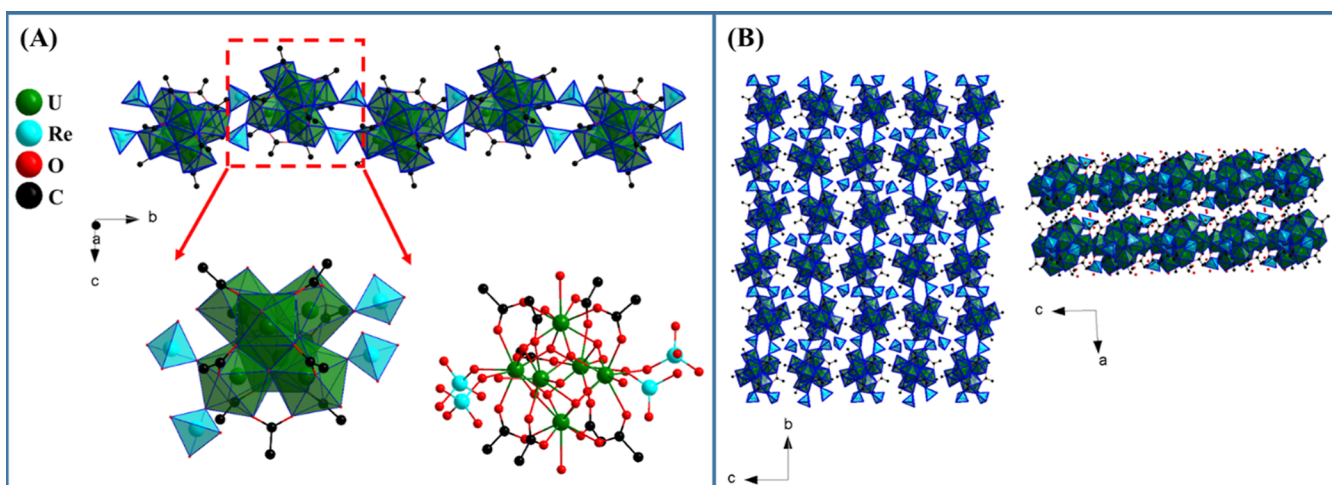


Figure 9. (A) Polyhedral representation of 1D chain $\text{U}^{\text{IV}}_6\text{Re}_3$ -chain viewed along different crystallographic planes. The polyhedral and ball-and-stick model exhibiting coordination of the U^{IV}_6 unit. Hydrogen atoms are omitted for clarity. (B) View down the a -axis highlighting the stacking of the layers in the a -direction.

$(\text{ReO}_4)_4(\text{H}_2\text{O})_3$. This framework is isostructural to previously reported Th(IV) and Pu(IV) compounds.^{11,12} The building block of this framework is a U(IV) metal center coordinated by nine oxygen atoms from six ReO_4^- and three H_2O (Figure 7A). Four of the six ReO_4^- groups bridge two U(IV)-polyhedra; two along the a -axis and two angled slightly out of the ac -plane. This leads to slightly corrugated layers in the ac plane which then stack in the b -direction (Figure 7B). The H-bonding ($\text{HOH}-\text{O}-\text{Re}$) and dispersion forces ($\text{Re}-\text{O}-\text{O}-\text{Re}$) hold the layers of frameworks together with observed $\text{O}-\text{O}$ interlayer distances around 2.7–3.0 Å. The average $\text{U}-\text{O}_{\text{w}}$ and $\text{U}-\text{O}_{\text{Re}}$ bond distances were 2.438 Å and 2.377, respectively. These bond distances are shorter than related $\text{Th}-\text{O}_{\text{w}}/\text{Th}-\text{O}_{\text{Re}}$ distances and longer than corollary $\text{Pu}-\text{O}_{\text{w}}/\text{Pu}-\text{O}_{\text{Re}}$, as expected from their periodic relationship (Table S2).

$\text{U}^{\text{IV}}_6\text{Re}_4^-$ 2D is 2D framework with hexanuclear U(IV) cluster (U^{IV}_6) prior isolated with different bridging/capping groups including sulfate, glycine, phosphate, carboxylate, pyridine, triflate, etc.^{22,24,34–39} as building block and has the moiety formula $\text{U}_6\text{O}_4(\text{OH})_4(\text{ReO}_4)_4(\text{CH}_3\text{COO})_8(\text{H}_2\text{O})_4$. In

the hexanuclear core (Figure 8A inset), six uranium atoms are arranged as a slightly distorted octahedron with U^{IV} bridged by eight μ_3 -O sites that cap the eight faces of the octahedron (Figure 8A). Previous studies suggested that in the U^{IV}_6 cluster, those eight μ_3 -O sites could be either all OH^- groups, or all O^{2-} groups, and frequently 50% OH^- and 50% O_2^- groups.^{17,40–42} Because of difficulties in locating the hydrogen atoms of these O sites and differentiating OH^- from O^{2-} groups directly from electron density map in the presence of heavy U atoms, those two groups were distinguished by the $\text{U}-\text{O}$ bond distance.^{39–42} In case of $\text{U}^{\text{IV}}_6\text{Re}_4^-$ 2D, four of the $\text{U}^{\text{IV}}-\text{O}$ bonds were longer with range in between 2.3894(50) and 2.4481(51) Å, similar to the literature value for the $\text{U}^{\text{IV}}-\mu_3-\text{OH}$ bond.¹⁷ The other four $\text{U}^{\text{IV}}-\text{O}$ bonds were shorter with range in between 2.2131(53) and 2.2538(50) Å, similar to the literature value for the $\text{U}^{\text{IV}}-\mu_3-\text{O}$ bond.¹⁷ Each of the U^{IV}_6 clusters is coordinated by eight ReO_4^- , eight CH_3COO^- , and four H_2O , and each U^{IV} is nine-coordinate. Each ReO_4^- bridges between two neighboring U(IV)-hexamers in the ab -plane, forming a 2D framework. The layers stack along the c -direction (Figure 8B). The crystalline structure also contains

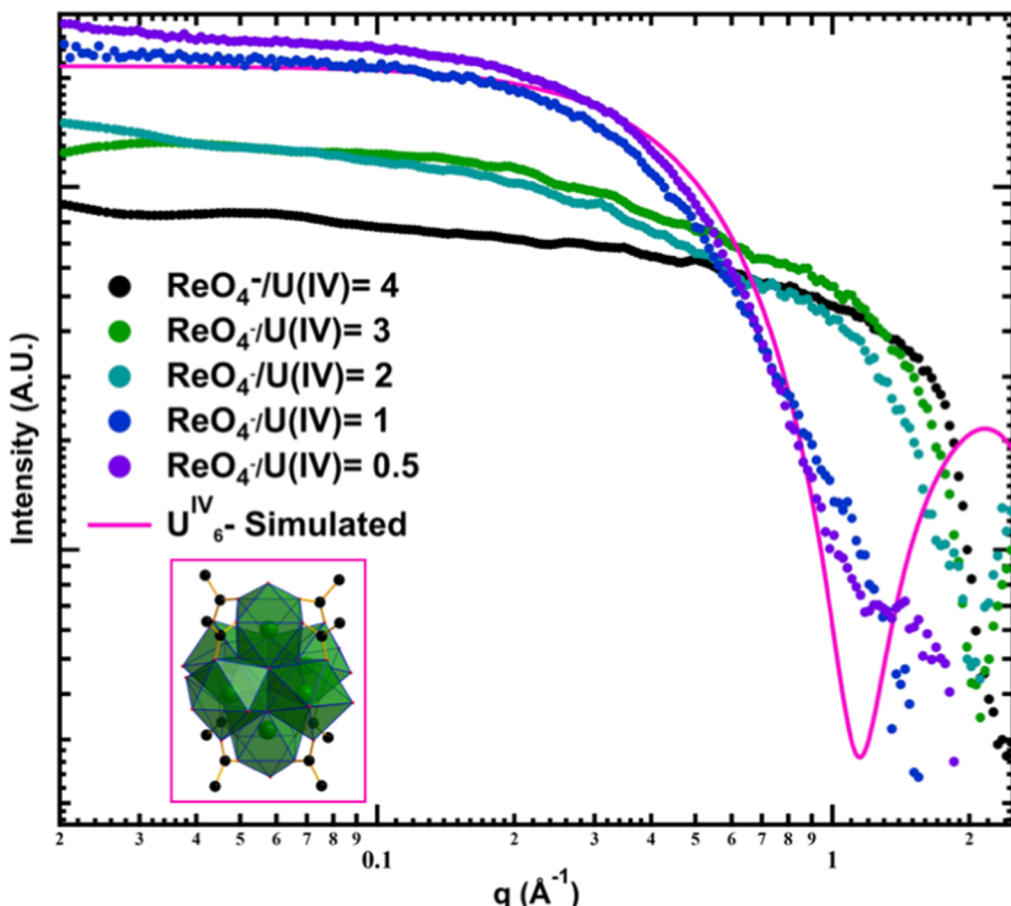


Figure 10. SAXS of uranium acetate and perrhenic acid reaction solutions.

water channels located between the layers. The water molecules (four per cluster unit) are likely H-bonded to uranium-bound water, with $\text{O}_{\text{water}}-\text{O}_{\text{water}}$ distance of 2.9055(16) Å.

The $\text{U}^{\text{IV}}_6\text{Re}_3$ -chain is an assemblage of U^{IV}_6 linked into chains, with a moiety formula $[\text{U}_6\text{O}_4(\text{OH})_4(\text{ReO}_4)_2(\text{CH}_3\text{COO})_9(\text{H}_2\text{O})_4](\text{ReO}_4)$ (Figure 9A). Six uranium atoms in the U^{IV}_6 core are bridged by four $\text{U}^{\text{IV}}-\mu_3-\text{OH}$ bonds with length between 2.3873(15) and 2.4539(12) Å and four $\text{U}^{\text{IV}}-\mu_3-\text{O}$ bonds with length in between 2.2013(11) and 2.2901 (12) Å (Figure 8A, inset). Each of the U^{IV}_6 cluster is coordinated by four ReO_4^- , nine CH_3COO^- , and six H_2O . Among six of the U(IV) in the U^{IV}_6 cluster, four are nine-coordinate and two are eight-coordinate, unlike $\text{U}^{\text{IV}}_6\text{Re}_4^-$ 2D where all the U(IV) are 9-coordinate. Each of the ReO_4^- are bridging ligands, connecting neighboring U^{IV}_6 hexamers along the *b*-axis to form a chain. The overall charge of this described unit is +1. The chains are further charge-balanced in the extended structure by free ReO_4^- anions located between layers of the chain in the *bc* plane (Figure 9B). The chains were stacked on top of each other along the *a*-axis. Partially occupied H-bonded solvent water molecules are also present between the stacked chain layers. The solvent water molecules are hydrogen-bonding with uranium-bonded $\text{H}_2\text{O}/\text{ReO}_4^-$ and free ReO_4^- with H-bond distances ranging from 2.7768(15) to 2.9755(18) Å.

3.3. Solution Characterization by SAXS. We performed SAXS analysis on reaction solutions with different $\text{ReO}_4^-/\text{U}(\text{IV})$ ratios (Figure 10 and Table 1) in order to determine if

Table 1. Details of Reaction Solution Used for SAXS Analysis

sample	concentration of ReO_4^- (mol/L)	concentration of U(IV) (mol/L)	$\text{ReO}_4^-/\text{U}(\text{IV})$ ratio	crystallized species
1	0.50	0.125	4	$\text{U}^{\text{IV}}\text{Re}_4^-$ 2D
2	0.50	0.167	3	$\text{U}^{\text{IV}}\text{Re}_4^-$ 2D
3	0.50	0.250	2	$\text{U}^{\text{IV}}\text{Re}_4^-$ 2D
4	0.50	0.50	1	$\text{U}^{\text{IV}}_6\text{Re}_4^-$ 2D
5	0.20	0.40	0.5	$\text{U}^{\text{IV}}_6\text{Re}_3$ chain

it is possible to observe the hexamer scattering in conditions in which ReO_4^- -linked hexamer frameworks crystallize. Because acetate serves the role of forming U(IV)-U(IV) bridges for hexamer formation instead of perrhenate, we do not expect the perrhenate to play a role in hexamer assembly. Additionally, excess perrhenic acid can prevent hexamer formation or disintegrate hexamers into monomers by protonation of the $\text{OH}^-/\text{O}^{2-}$ bridges in the highly acidic media. We did not measure SAXS on U(IV) acetate alone due to poor solubility. Therefore, perrhenic acid, even the lowest concentration used in this study, enabled dissolution. The SAXS curves for reaction solutions with ratios $\text{ReO}_4^-/\text{U}(\text{IV}) = 2$ to 4 are weakly scattering with a “bump” at high-*q*, around $q \sim 1.5 \text{ \AA}^{-1}$. Prior experience with perrhenate systems indicates that this represents free ReO_4^- in solution.^{14,15} X-ray absorption by the heavy metals also leads to observed weak scattering. At smaller $\text{ReO}_4^-/\text{U}(\text{IV})$ ratios, with both reduced acidity and less interference from free ReO_4^- scattering, a well-defined

Guinier elbow becomes apparent from $q \sim 0.1\text{--}0.6 \text{\AA}^{-1}$, that is similar to that of a simulated hexamer scattering (Figure 10). In summary, these analyses suggest the U(IV) acetate dissolves as acetate-bridged hexamers and may also explain its poor solubility without added acid. These lower acid conditions (Table 1) are also the conditions from which ReO_4^- -linked U^{IV}_6 -hexamer phases were crystallized.

The SAXS analysis of U(VI) reaction solutions at different metal to oxoanion ratios has been reported in our previous work.¹³ In those studies, the reaction solutions showed a relatively weak scattering. The particle size was consistent with monomeric species instead of intact clusters since uranyl does not exhibit similar hydrolysis behavior as U^{IV} .

3.4. Additional Characterization of Crystalline Materials. Bulk characterization including FTIR, PXRD, and SEM-EDS was performed on the perrhenate crystals. However, TcO_4^- -containing material characterization was limited to SEM-EDS due to the potential for radioactive contamination of the various instruments.

The FTIR spectra of crystalline materials from different phases show two broad peaks centered at $\sim 920 \text{ cm}^{-1}$ and $\sim 840 \text{ cm}^{-1}$ within the $970\text{--}750 \text{ cm}^{-1}$ region, associated with stretching of UO_2 and ReO_4^- groups.^{8,43,44} The OH stretching and H_2O bending vibration are indicated by peaks in the region $3700\text{--}3050 \text{ cm}^{-1}$ and $1705\text{--}1530 \text{ cm}^{-1}$. $\text{U}^{\text{IV}}_6\text{Re}_4^-$ 2D and $\text{U}^{\text{IV}}_6\text{Re}_3^-$ chain show additional peaks related to CH_3COO^- groups that are assigned in Table S3.

The PXRD patterns of crystalline material belonging to different phases match well with the calculated pattern from elucidated structures (Figures S2 and S3). However, preferred crystallographic orientation have been observed in experimental patterns which created mismatch in relative intensity. Furthermore, in case of the U(VI) system, we have observed crystallization of the minor phase along with the major phase. The minor phases may contribute to evolution of small peaks in the pattern. These made it difficult to assign some peaks when compared with calculated pattern.

The SEM analysis of the crystalline materials from different phases shows crystals with either blocky or plate-like morphologies (Figures S4–S12). The EDS analyses show all the expected elements (Figures S4–S12). The atomic ratio between Re/U and Tc/U (calculated by EDS analysis of the different phases) is consistent (except $\text{U}^{\text{VI}}\text{Re}_2^-$ chain) with the formulas determined by SCXRD (Tables S4–S13). The inconsistency in the atomic ratio between EDS and SCXRD analysis is likely related to the presence of minor phases and byproduct crystals, including pertechnic/perrhenic acid.

The Raman spectra of crystals isolated from ReO_4^- and U(IV) solutions are dominated by the vibrational modes of perrhenate (Figure S13). The wide band in between 305 and 382 cm^{-1} is the bending modes of ReO_4^- .⁴⁵ The symmetric stretch (ν_1) and antisymmetric stretch (ν_3) of ReO_4^- are observed at $960\text{--}998$ and $830\text{--}865 \text{ cm}^{-1}$, respectively.⁴³

The UV-visible spectra of mother liquor from U(VI)/ TcO_4^- and U(IV)/ ReO_4^- have shown a wide and intense characteristic band of $\text{ReO}_4^-/\text{TcO}_4^-$ species in between 200 and 300 nm due to fine-structured charge transfer (Figure S14).⁴⁶

4. CONCLUSION

This work contributes to our growing understanding of coordination chemistry between $\text{Tc}^{\text{VII}}\text{-99}$ oxoanions (plus nonradioactive surrogate ReO_4^-) and uranium, which coexist

in SNF and legacy nuclear wastes. We demonstrate that for both $\text{U}^{\text{VI}}\text{O}_2^{2+}$ and U(IV), higher pertechnic/perrhenic acid concentrations yield one and two-dimensional phases with monomeric uranium linked by $\text{ReO}_4^-/\text{TcO}_4^-$, while lower concentrations yield frameworks based on uranyl and U(IV) clusters. With ReO_4^- as the connecting oxoanion, the classic $\text{U}^{\text{IV}}_6\text{O}_4(\text{OH})_4^{12-}$ oxocation with bridging acetates from the uranium(IV) acetate source self-assembles, also in one-dimensional and 2-dimensional frameworks. This hexamer is common to all the tetravalent actinides (Zr^{IV} , Hf^{IV} , Np^{IV} , Pu^{IV}), best known in the UiO-66 metal-organic framework, and also the same core building block as simple fluorite-type $\text{M}^{\text{IV}}\text{O}_2$ oxide. SAXS studies show that U^{IV} is dissolved in the hexamer form in reaction solutions from which these phases crystallize, perhaps explaining the universally poor solubility of U^{IV} acetate. In the described experiments, $\text{U}^{\text{IV}}\text{-TcO}_4^-$ phases were not crystallized, which was challenged by the reduction of technetium and oxidation of uranium. However, this represents opportunity to obtain oxoclusters with reduced technetium (which favors cluster assembly) and either U^{IV} or U^{VI} , such as our prior reported $[(\text{U}^{\text{VI}}\text{O}_2)_4(\text{Tc}^{\text{V}}\text{O})(\text{O})_4(\text{CH}_3\text{COO})_4(\text{H}_2\text{O})_4]$.¹³ Isolation of $\text{U}^{\text{IV}}\text{-TcO}_4^-$ or $\text{U}^{\text{IV}}\text{-Tc}^{\text{IV/V}/\text{VI}}$ will require harnessing control over redox chemistry and synthesis in more reducing conditions for the latter. If achievable, this goal will enable important fundamental and applied scientific information for this system.

■ ASSOCIATED CONTENT

SI Supporting Information

The Supporting Information is available free of charge at <https://pubs.acs.org/doi/10.1021/acs.inorgchem.Sc01958>.

Additional details and images of SCXRD, FTIR, PXRD, SEM-EDS, Raman spectra, and UV-vis analysis (PDF)

Accession Codes

The crystalline structures are deposited in CCDC database and can be requested by deposition number 2445905–2445915.

■ AUTHOR INFORMATION

Corresponding Authors

Mohammad Shohel – Department of Chemistry, Oregon State University, Corvallis, Oregon 97331, United States; Present Address: Mohammad Shohel—Sandia National Laboratories, Albuquerque, NM-87185, USA;
ORCID: [0000-0003-2736-2389](https://orcid.org/0000-0003-2736-2389); Email: mshohel@sandia.gov

May Nyman – Department of Chemistry, Oregon State University, Corvallis, Oregon 97331, United States;
ORCID: [0000-0002-1787-0518](https://orcid.org/0000-0002-1787-0518); Email: may.nyman@oregonstate.edu

Author

Ian Colliard – Department of Chemistry, Oregon State University, Corvallis, Oregon 97331, United States; Present Address: Ian Colliard—Lawrence Livermore National Laboratory, Livermore, California 94550, United States.

Complete contact information is available at:
<https://pubs.acs.org/10.1021/acs.inorgchem.Sc01958>

Author Contributions

The manuscript was written through contributions of all authors. All authors have contributed toward writing the manuscript and have given approval to the final version of the

manuscript. M.N. and M.S. conceptualized the study. M.N. provided funding, guidance, and supervised the study. M.S. carried out all the synthesis, characterization, and wrote the first draft of the manuscript. I.C. carried out some initial synthesis and isolated one of the compounds.

Notes

The authors declare no competing financial interest.

ACKNOWLEDGMENTS

This study was supported by the Department of Energy, National Nuclear Security Administration under Award DE-NA0003763. We acknowledge the Murdock Charitable Trust (grant SR-2017297) for acquisition of the SCXRD. The isotope ($Tc-99$) used in this research was supplied by the U.S. Department of Energy Isotope Program, managed by the Office of Isotope R&D and Production.

REFERENCES

- (1) Irish, E. R.; Reas, W. H. *The Purex Process—A Solvent Extraction Reprocessing Method for Irradiated Uranium; HW-49483 A; General Electric Co. Hanford Atomic Products Operation*; Richland, Wash: United States, 1957.
- (2) Law, J. D. Aqueous Reprocessing of Used Nuclear Fuel. *World Sci.* Hackensack, NJ, USA. **2018**, 1.
- (3) Moeyaert, P.; Dumas, T.; Guillaumont, D.; Kvashnina, K.; Sorel, C.; Migurditchian, M.; Moisy, P.; Dufrêche, J.-F. Modeling and Speciation Study of Uranium(VI) and Technetium(VII) Coextraction with DEHiBA. *Inorg. Chem.* **2016**, 55 (13), 6511–6519.
- (4) John, G. H.; May, I.; Sharrad, C. A.; Sutton, A. D.; Collison, D.; Helliwell, M.; Sarsfield, M. J. The Synthesis, Structural, and Spectroscopic Characterization of Uranium(IV) Perrhenate Complexes. *Inorg. Chem.* **2005**, 44 (21), 7606–7615.
- (5) Sutton, A. D.; May, I.; Sharrad, C. A.; Sarsfield, M. J.; Helliwell, M. The coordination of perrhenate and pertechnetate to thorium(IV) in the presence of phosphine oxide or phosphate ligands. *Dalton Trans.* **2006**, No. 48, 5734–5742.
- (6) John, G. H.; May, I.; Sarsfield, M. J.; Collison, D.; Helliwell, M. Dimeric uranyl complexes with bridging perrhenates. *Dalton Trans.* **2007**, No. 16, 1603–1610.
- (7) Fedosseev, A. M.; Budantseva, N. A.; Grigoriev, M. S.; Guerman, K. E.; Krupa, J.-C. Synthesis and properties of neptunium(VI,V) and plutonium(VI) pertechnetates. *Radiochim. Acta* **2003**, 91 (3), 147–152.
- (8) Karimova, O. V.; Burns, P. C. Structural Units in Three Uranyl Perrhenates. *Inorg. Chem.* **2007**, 46 (24), 10108–10113.
- (9) Decoteau, E. A.; Polinski, M. J. Synthesis and characterization of new families of lanthanide perrhenate complexes. *J. Solid State Chem.* **2022**, 306, 122780.
- (10) Strub, E.; Grödler, D.; Zaratti, D.; Yong, C.; Dünnbier, L.; Bazhenova, S.; Roca Jungfer, M.; Breugst, M.; Zegke, M. Pertechnetates – A Structural Study Across the Periodic Table. *Chem. - Eur. J.* **2024**, 30 (26), No. e202400131.
- (11) Shohel, M.; Bustos, J.; Stroscio, G. D.; Sarkar, A.; Nyman, M. Elucidating Actinide–Pertechnetate and Actinide–Perrhenate Bonding via a Family of $Th-TcO_4$ and $Th-ReO_4$ Frameworks and Solutions. *Inorg. Chem.* **2023**, 62 (26), 10450–10460.
- (12) Shohel, M.; Sockwell, A. K.; Hixon, A. E.; Nyman, M. Plutonium and Cerium Perrhenate/Pertechnetate Coordination Polymers and Frameworks. *Inorg. Chem.* **2024**, 63 (4), 2044–2052.
- (13) Shohel, M.; Nyman, M. Uranyl- $Tc(VII)/Tc(V)$ hybrid clusters. *Chem. Commun.* **2024**, 60 (45), 5820–5823.
- (14) Shohel, M.; Bustos, J.; Roseborough, A.; Nyman, M. Pertechnetate/perrhenate-capped Zr/Hf -Dihydroxide Dimers: Elucidating $Zr-TcO_4$ Co-Mobility in the Nuclear Fuel Cycle. *Chem. - Eur. J.* **2024**, 30 (10), No. e202303218.
- (15) Bustos, J.; Shohel, M.; Buzanich, A. G.; Zakharov, L.; Buils, J.; Segado-Centellas, M.; Bo, C.; Nyman, M. Technetium and Rhenium Auto-reduction, Polymerization and Lability towards Group VII Polyoxometalate Chemistry. *Chem. - Eur. J.* **2025**, 31 (21), No. e202404144.
- (16) Martin, N. P.; Volkringer, C.; Henry, N.; Trivelli, X.; Stoclet, G.; Ikeda-Ohno, A.; Loiseau, T. Formation of a new type of uranium(IV) poly-oxo cluster $\{U_{38}\}$ based on a controlled release of water via esterification reaction. *Chem. Sci.* **2018**, 9 (22), 5021–5032.
- (17) Knope, K. E.; Soderholm, L. Solution and Solid-State Structural Chemistry of Actinide Hydrates and Their Hydrolysis and Condensation Products. *Chem. Rev.* **2013**, 113 (2), 944–994.
- (18) Colliard, I.; Morrison, G.; zur Loye, H.-C.; Nyman, M. Supramolecular Assembly of U(IV) Clusters and Superatoms with Unconventional Counterions. *J. Am. Chem. Soc.* **2020**, 142 (19), 9039–9047.
- (19) McCusker, T. L.; Vanagas, N. A.; Szymanowski, J. E. S.; Surbella, R. G.; Bertke, J. A.; Arteaga, A.; Knope, K. E. Elucidating trends in synthesis and structural periodicity in a series of tetravalent actinide–oxo hexamers. *CrystEngComm* **2025**, 27 (4), 507–515.
- (20) Qiu, J.; Burns, P. C. Clusters of Actinides with Oxide, Peroxide, or Hydroxide Bridges. *Chem. Rev.* **2013**, 113 (2), 1097–1120.
- (21) Tamain, C.; Dumas, T.; Hennig, C.; Guilbaud, P. Coordination of Tetravalent Actinides ($An = Th^{IV}, U^{IV}, Np^{IV}, Pu^{IV}$) with DOTA: From Dimers to Hexamers. *Chem. - Eur. J.* **2017**, 23 (28), 6864–6875.
- (22) Falaise, C.; Neal, H. A.; Nyman, M. U(IV) Aqueous Speciation from the Monomer to UO_2 Nanoparticles: Two Levels of Control from Zwitterionic Glycine Ligands. *Inorg. Chem.* **2017**, 56 (11), 6591–6598.
- (23) Grdenić, D.; Korpar-Čolig, B. Uranium(IV) acetate and its double acetates with magnesium, iron, and zinc. *J. Inorg. Nucl. Chem.* **1968**, 30 (7), 1751–1755.
- (24) Colliard, I.; Falaise, C.; Nyman, M. Bridging the Transuranics with Uranium(IV) Sulfate Aqueous Species and Solid Phases. *Inorg. Chem.* **2020**, 59 (23), 17049–17057.
- (25) Salomone, V. N.; Meichtry, J. M.; Schinelli, G.; Leyva, A. G.; Litter, M. I. Photochemical reduction of U(VI) in aqueous solution in the presence of 2-propanol. *J. Photochem. Photobiol., A* **2014**, 277, 19–26.
- (26) SAINT Plus, Version 8.34a; Bruker AXS Inc.: Madison, Wisconsin, 2013.
- (27) Sheldrick, G. M. *Bruker-Siemens area Detector. Absorb. other Correct*, Version 2008/12008.
- (28) Sheldrick, G. SHELXT - Integrated space-group and crystal-structure determination. *Acta Crystallogr., Sect. A* **2015**, 71 (1), 3–8.
- (29) Sheldrick, G. A. short history of SHELX. *Acta Crystallogr., Sect. A* **2008**, 64 (1), 112–122.
- (30) Dolomanov, O. V.; Bourhis, L. J.; Gildea, R. J.; Howard, J. A. K.; Puschmann, H. OLEX2: a complete structure solution, refinement and analysis program. *J. Appl. Crystallogr.* **2009**, 42 (2), 339–341.
- (31) Ilavsky, J.; Jemian, P. R. Irena: tool suite for modeling and analysis of small-angle scattering. *J. Appl. Crystallogr.* **2009**, 42 (2), 347–353.
- (32) Zuo, X.; Cui, G.; Merz, K. M.; Zhang, L.; Lewis, F. D.; Tiede, D. M. X-ray diffraction “fingerprinting” of DNA structure in solution for quantitative evaluation of molecular dynamics simulation. *Proc. Natl. Acad. Sci. U.S.A.* **2006**, 103 (10), 3534–3539.
- (33) Mihalcea, I.; Henry, N.; Volkringer, C.; Loiseau, T. Uranyl-Pyromellitate Coordination Polymers: Toward Three-Dimensional Open Frameworks with Large Channel Systems. *Cryst. Growth Des.* **2012**, 12 (1), 526–535.
- (34) Lundgren, G. The crystal structure of $U_6O_4(OH)_4(SO_4)_6$. *Ark. Kemi.* **1953**, 5 (4), 349–363.
- (35) Duval, P. B.; Burns, C. J.; Clark, D. L.; Morris, D. E.; Scott, B. L.; Thompson, J. D.; Werkema, E. L.; Jia, L.; Andersen, R. A. Synthesis and Structural Characterization of the First Uranium Cluster Containing an Isopolyoxometalate Core. *Angew. Chem., Int. Ed.* **2001**, 40 (18), 3357–3361.

- (36) Mokry, L. M.; Dean, N. S.; Carrano, C. J. Synthesis and Structure of a Discrete Hexanuclear Uranium–Phosphate Complex. *Angew Chem. Int. Ed. Engl.* **1996**, *35* (13–14), 1497–1498.
- (37) Berthet, J.-C.; Thuéry, P.; Ephritikhine, M. Unprecedented reduction of the uranyl ion $[\text{UO}_2]^{2+}$ into a polyoxo uranium(IV) cluster: Synthesis and crystal structure of the first f-element oxide with a $\text{M}_6(\mu_3\text{O})_8$ core. *Chem. Commun.* **2005**, *27*, 3415–3417.
- (38) Colliard, I.; Brown, J. C.; Nyman, M. Metal–Oxo Cluster Formation Using Ammonium and Sulfate to Differentiate M^{IV} (Th, U, Ce) Chemistries. *Inorg. Chem.* **2023**, *62* (5), 1891–1900.
- (39) Falaise, C.; Volkrieger, C.; Loiseau, T. Mixed Formate-Dicarboxylate Coordination Polymers with Tetravalent Uranium: Occurrence of Tetranuclear $\{\text{U}_4\text{O}_4\}$ and Hexanuclear $\{\text{U}_6\text{O}_4(\text{OH})_4\}$ Motifs. *Cryst. Growth Des.* **2013**, *13* (7), 3225–3231.
- (40) Murray, A. V.; Wacker, J. N.; Bertke, J. A.; Knope, K. E. Synthesis, Characterization, and Solid-State Structural Chemistry of Uranium(IV) Aliphatic Dicarboxylates. *Cryst. Growth Des.* **2021**, *21* (4), 2429–2444.
- (41) Ling, J.; Lu, H.; Wang, Y.; Johnson, K.; Wang, S. One-dimensional chain structures of hexanuclear uranium(IV) clusters bridged by formate ligands. *RSC Adv.* **2018**, *8* (61), 34947–34953.
- (42) Mougel, V.; Biswas, B.; Pécaut, J.; Mazzanti, M. New insights into the acid mediated disproportionation of pentavalent uranyl. *Chem. Commun.* **2010**, *46* (45), 8648–8650.
- (43) Chakravorti, M. C. The chemistry of coordinated perrhenate (ReO_4^-). *Coord. Chem. Rev.* **1990**, *106*, 205–225.
- (44) Lu, G.; Haes, A. J.; Forbes, T. Z. Detection and identification of solids, surfaces, and solutions of uranium using vibrational spectroscopy. *Coord. Chem. Rev.* **2018**, *374*, 314–344.
- (45) Busey, R. H.; Keller, O. L., Jr. Structure of the Aqueous Pertechnetate Ion by Raman and Infrared Spectroscopy. Raman and Infrared Spectra of Crystalline KTcO_4 , KReO_4 , Na_2MoO_4 , Na_2WO_4 , $\text{Na}_2\text{MoO}_4 \cdot 2\text{H}_2\text{O}$, and $\text{Na}_2\text{WO}_4 \cdot 2\text{H}_2\text{O}$. *J. Chem. Phys.* **1964**, *41* (1), 215–225.
- (46) Said, K. B.; Fattah, M.; Musikas, C.; Delorme-Hiver, A.; Abbé, J. C. A Novel Approach to the Oxidation Potential of the $\text{Tc(VII)}/\text{Tc(IV)}$ Couple in Hydrochloric Acid Medium through the Reduction of TcO_4^- Ion. *Radiochim. Acta* **1998**, *83* (4), 195–204.

CAS BIOFINDER DISCOVERY PLATFORM™

**PRECISION DATA
FOR FASTER
DRUG
DISCOVERY**

CAS BioFinder helps you identify targets, biomarkers, and pathways

Unlock insights

CAS
A division of the
American Chemical Society